ELSEVIER

Physics of the Earth and Planetary Interiors 123 (2001) 205–219

PHYSICS OF THE EARTH AND PLANETARY INTERIORS

www.elsevier.com/locate/pepi

Crust and upper mantle P- and S-wave delay times at Eurasian seismic stations

E.R. Engdahl*, M.H. Ritzwoller

Center for Imaging the Earth's Interior, Department of Physics, University of Colorado, Boulder, CO 80309-0390, USA

Abstract

Median crust and upper mantle P- and S-wave delay times, based on residuals for teleseismic P- and S-wave arrival times included in the groomed ISC/NEIC database of Engdahl et al. [Bull. Seism. Soc. Am. 88 (1998) 722] are estimated as functions of time and azimuth for Eurasian seismic stations. The effects of source and lower mantle 3-D structure on the station residuals are corrected by ray tracing all phase data (to a depth of 400 km below the station) through the 3-D P- and S-wave models of Bijwaard et al. [J. Geophys. Res. 103 (1998) 30055] and Bijwaard [Seismic travel-time tomography for detailed global mantle structure. University of Utrecht, Utrecht, The Netherlands, 1999, 179 pp.], respectively. In general, crust and upper mantle P- and S-station delays based on medians of azimuthally binned residuals are spatially coherent and can be qualitatively associated with Eurasian tectonic features such as orogens and cratons, as well as with structural elements such as sediment and crustal thickness, and average uppermost mantle velocities. Paired P- and S-station delays are correlated with a rather poorly determined slope (S/P delay time ratio) of about 1.9.

Keywords: Eurasia; Seismic stations; Body waves; Delay times; Crust; Upper mantle

1. Introduction

We present in this paper crust and upper mantle P- and S-wave delay times at Eurasian seismic stations. Our primary motivation for conducting this study is to use these data to calibrate and/or validate 3-D models being developed for Eurasia (e.g. Villasenor et al., 2000) in order to improve seismic event location. For example, if we can reliably estimate the S/P delay time ratio and provided that the S- and P-velocities are correlated, these data can be used to construct a hybrid P-velocity model for the Eurasian crust and upper mantle directly from an S-model. Moreover, if the effects of upper mantle structure on P- and S-station delays beneath Eurasia can be isolated, we can use that information to assess the validity of features of any of the 3-D models being developed. We can also use our analyses of station delays to identify "surrogate" stations, that is stations operating before 1995 that are near stations of the International Monitoring System (IMS) and that can be used to extend the ground truth data base to the earlier period.

The challenge of this study is to estimate reliably crust and upper mantle P- and S-wave delay times using residuals for phase arrival times from globally occurring events routinely reported by seismic stations to international agencies. To achieve this goal there are a number of factors that need to be taken into account. For example, the characteristics of routinely reported data are highly non-uniform. Large variations in phase residuals, such as shifts or

* Corresponding author. Fax: +1-303-492-7935.
E-mail address: engdahl@colorado.edu (E.R. Engdahl).

0031-9201/01/$ – see front matter
PII: S0031-9201(00)00210-7

drifts in time, can be caused by poor timing accuracy, equipment changes, biased picking of arrival times, or even unreported changes in station location (Roehm et al., 1999). The distribution of residuals in time for a station can also be strongly affected by spatial and temporal variations in earthquake occurrence globally. Finally, procedures need to be developed that can minimize these effects and produce meaningful statistics.

In this paper, we first investigate the stability of phase reporting in time for each station and use our approach to address the surrogate station problem. Next we attempt to identify the source of observed azimuthal anomalies and to isolate the true delay caused by the upper mantle beneath each station by correcting all of the phase residual data for 3-D structure outside this region of interest. These analyses are made possible by using robust estimates of median station delays based on a scheme that bins all phase residual data azimuthally. We examine the final corrected P- and S-median station delays to over 300 Eurasian

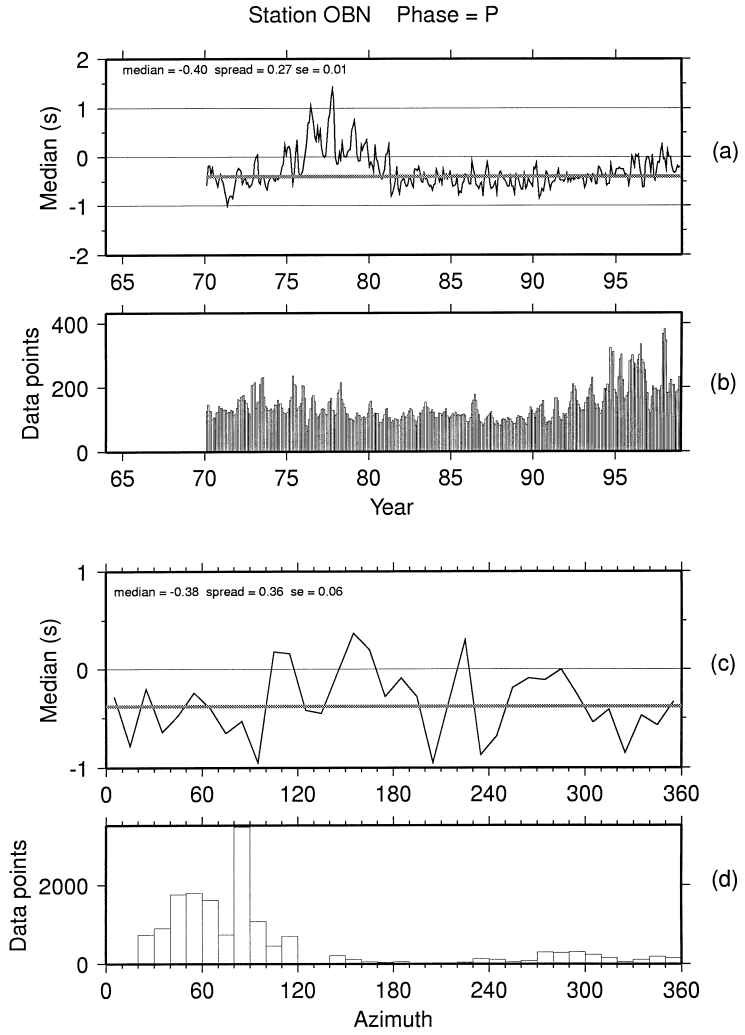

Fig. 1. (a) Monthly grand medians of teleseismic P-residual medians observed at station OBN taken over 20° azimuth sectors within a 3-month moving window and plotted on the middle month. (b) Number of teleseismic P-residuals per year. (c) Azimuthal P-residual medians plotted over 10° azimuth sectors. (d) Number of teleseismic P-residuals per azimuth sector.

stations for spatial coherence and correlation to tectonic features, and to structural elements of a new 3-D uppermost mantle model for central Eurasia developed from surface wave data (Villasenor et al., 2000).

2. Methodology

2.1. Data selection

We select residual data only at teleseismic distances because at regional distances the effects of 3-D lateral heterogeneity are difficult to separate from the upper mantle signal beneath the station that we are trying to isolate. The effects of 3-D structure are further exacerbated by the considerable spatial and temporal variation in the occurrence of earthquakes regionally. Basically, teleseismic ray paths to stations are nearly vertical and the onset of phase picks are less complicated and/or ambiguous, making these data ideal for estimation of station delays that can be correlated with 3-D models.

We use a "groomed" phase data base of well-constrained teleseismic events that occurred during the period 1964–1999 (Engdahl et al., 1998) to examine teleseismic residuals for P- and S-phases reported to

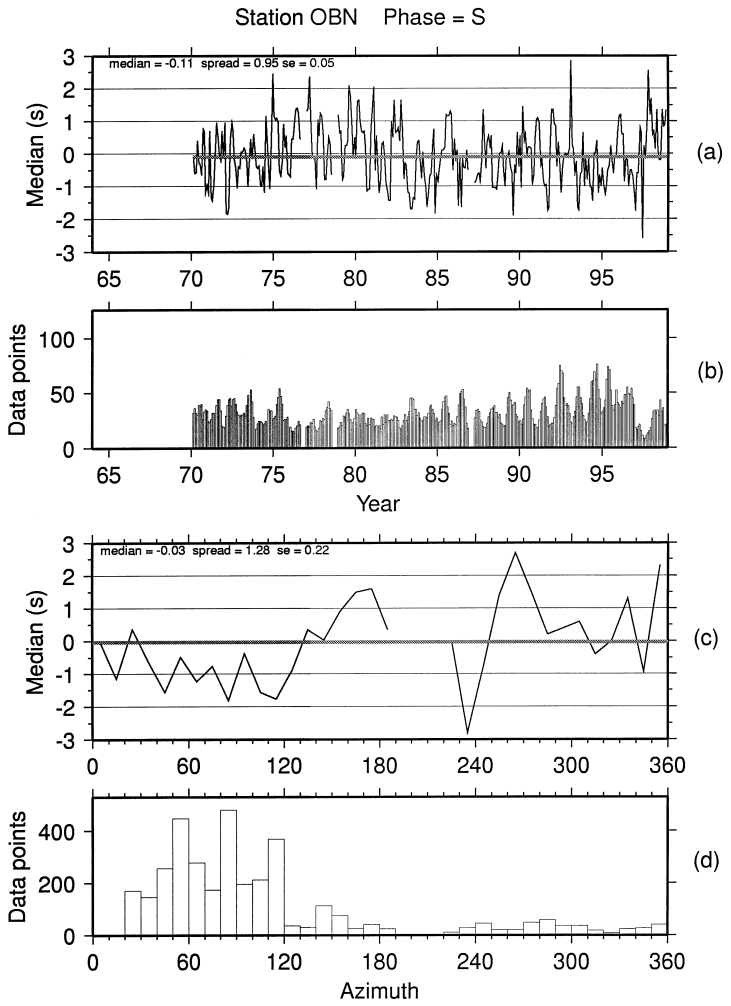

Fig. 2. Same as Fig. 1 but for teleseismic S-residual medians observed at station OBN.

the ISC/NEIC by Eurasian stations. Only teleseismic P- and S-arrivals that bottom in the lower mantle were selected for processing. Rays for P-waves must bottom between depths of 740 and 2740 km (the top of the D″ layer in model ak135) and for S-waves between depths of 760 and 2740 km. These rays correspond to surface focus distances of 28° and 91° for P-waves and 27° and 94° for S-waves. These criteria ensure that all phase data selected are at or beyond the triplication cusp from the 660 discontinuity and do not pass through the D″ layer. Within the selected distance ranges the observed spread of the median travel time residual (defined later) is less than 1.21 s for P-phases and 3.20 s for S-phases.

2.2. Robust statistics

The station residual data base contains a large number of outliers, thereby necessitating a robust median statistics approach using an algorithm programmed by R. Buland (personal communication). We implement this algorithm by grouping travel time residuals (relative to ak135) into bins of size 0.1 s (the reported precision of most data) using ranges of ±5.0 s for P-phases

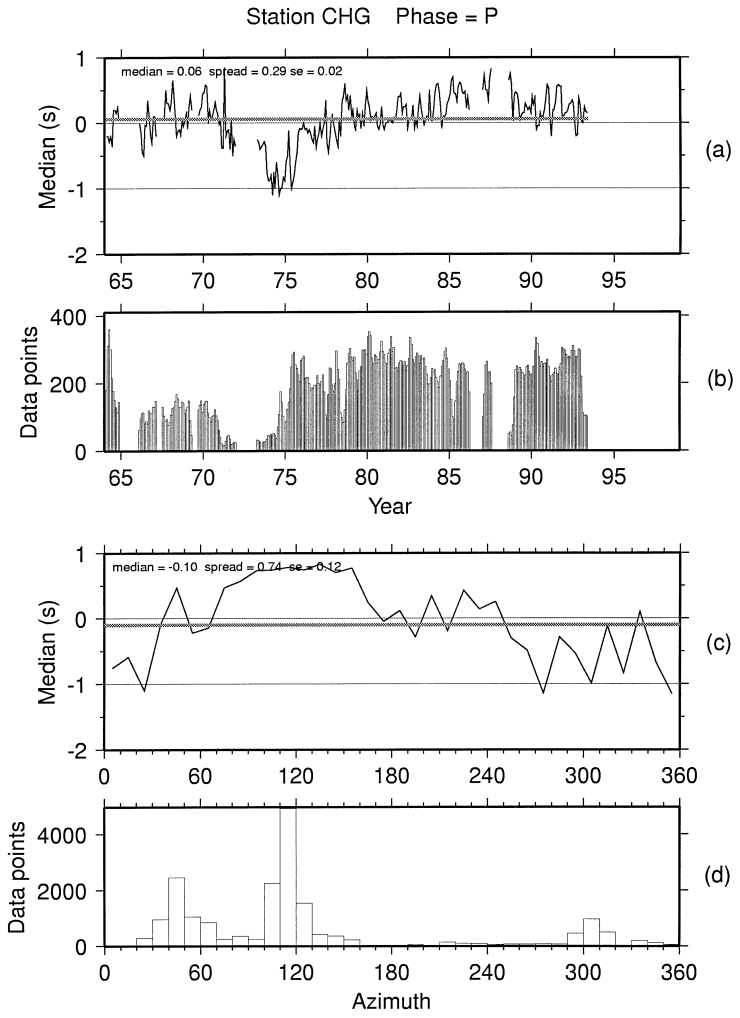

Fig. 3. Same as Fig. 1 but for teleseismic P-residual medians observed at station CHG (Chang Mai, Thailand).

and ±15.0 s for S-phases. Estimating the median from binned groups is highly efficient, and robust estimates of the median and the spread are determined from the grouped data. The spread is defined as the median of the absolute differences between the residuals and the median residual scaled to yield one S.D. when applied to a Gaussian distribution. The S.E. of the median is estimated by dividing the spread by the square root of the total number of binned observations. To remove a modest number of outliers median data for a station are not used if the spread and standard error are greater than 1.0 and 0.3 s if based on P-wave residuals and 1.3 and 0.4 s if based on S-wave residuals.

2.3. Station time history

The time history of reported station residuals is examined by estimating median station residuals for teleseismic P- and S-phases as a function of time. This is accomplished by binning residuals in 20° azimuth sectors over a 3-month window that moves in time, estimating the median in each sector, and then assigning the grand median of all sector medians to the central month of that window. The binning sizes of azimuth sectors and time windows were chosen so as to optimize the distribution and number of station residual data in each bin. The only constraint imposed is that

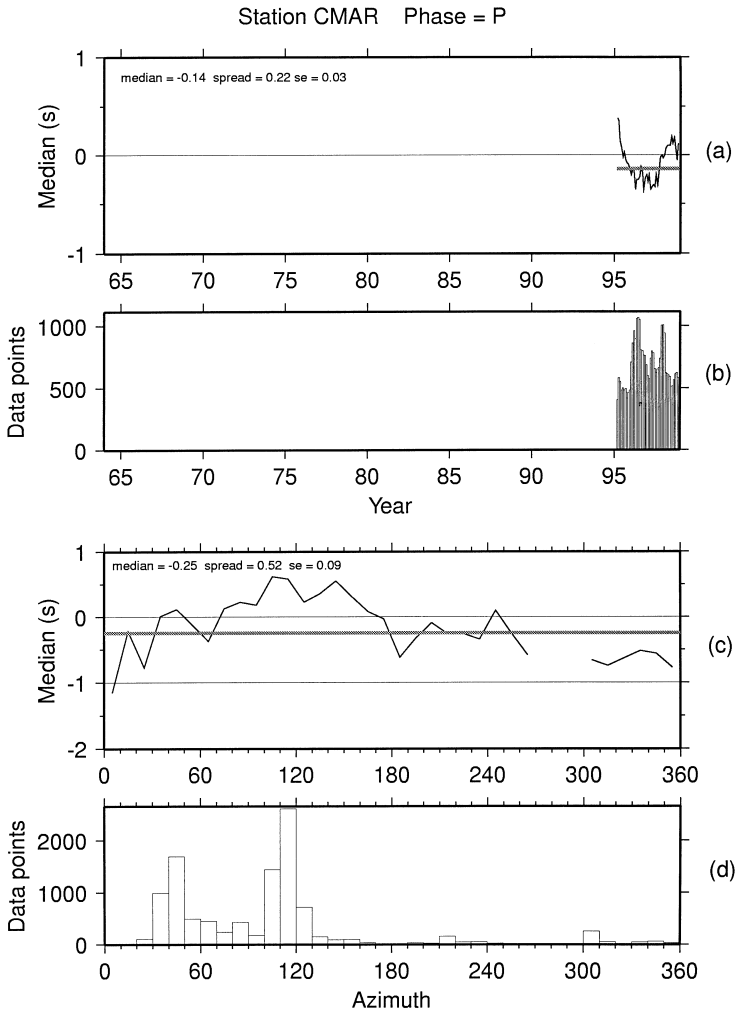

Fig. 4. Same as Fig. 1 but for teleseismic P-residual medians observed at station CMAR (Chang Mai Array, Thailand).

there cannot be more than nine adjacent empty sectors (180° azimuth gap) for a grand median to be estimated. This approach strongly reduces the effects of uneven sampling caused by the location of stations relative to active seismic source zones at teleseismic distances.

Fig. 1(a) shows is a typical example of a station with a long reporting history for which the moving window median of P-residuals has some prominent fluctuations in time. For station Obninsk (OBN), there is a large positive excursion in the median estimates between about 1976 and 1980, as well as a slight positive offset after 1995. To date the operators of station OBN have not provided the authors with an explanation for these fluctuations. Nevertheless, for this example of a short-term variation in time the grand median of the monthly medians appears to be only slightly biased (−0.40 with a spread of 0.27 and S.E. of 0.01). Residuals are also examined as a function of their azimuth by binning all residuals in time into 10° azimuth sectors, estimating the median in each sector, and then determining the grand median of all sector medians with the same constraint on azimuth gap as used above. For station OBN the grand median of the sector medians shown in Fig. 1(c) is −0.38 (with a spread of 0.36 and S.E. of 0.06). Thus, when fluctuations in time are short term it is possible to make stable estimates of the grand median of P-residuals in both time and azimuth. Also shown in Fig. 1 are the number of data points per month (Fig. 1(b)) and by azimuth sector (Fig. 1(d)). Without the binning procedures described above, data from sources in the azimuth range of 80–90° would dominate the estimates of station delays.

Fig. 2 show similar plots in time and azimuth for median S-residuals reported by station OBN. Not unexpectedly, the median scatter is larger in both time and azimuth. Grand medians in time and azimuth are −0.11 (with a spread of 0.95 and S.D. of 0.05) and −0.03 (with a spread of 1.28 and a standard error of 0.22), respectively. Although somewhat obscured by the different scaling, the same fluctuation in time (between 1976 and 1980) seen for P-residual medians in Fig. 1(a) can also be seen in Fig. 2(a) Moreover, the shapes of the azimuthal median plots for P and S (Figs. 1(c) and 2(c)) are quite similar, suggesting that the structural effects being mapped into the azimuthal sector medians are the same.

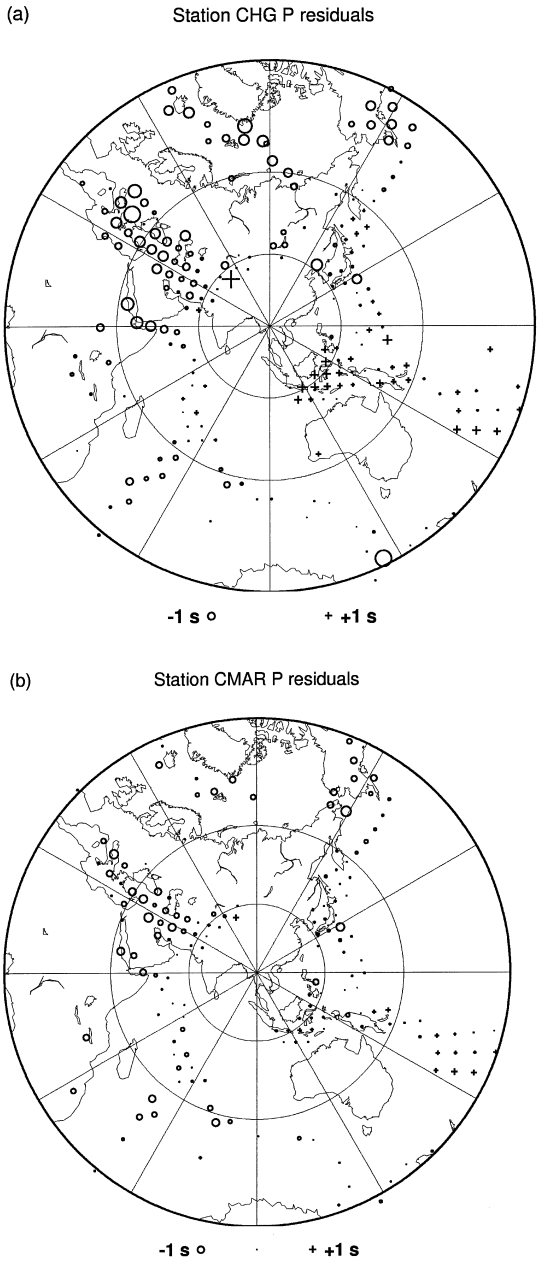

Fig. 5. Source patch (5° × 5° grid) medians of residuals for P-rays bottoming in the lower mantle observed at stations (a) CHG and (b) CMAR.

2.4. Surrogate stations

As a test of how well station time and azimuth medians are resolved we address the surrogate station problem. Most primary and auxiliary IMS seismic stations are located at or near the sites of conventional stations that have a long reporting history. Preliminary analysis of stations potentially surrogate to IMS stations globally suggests that for most regions unique historical reference events recorded by surrogate stations can be used to calibrate stations of the IMS network, provided that the separation distances are no more than 100 km and differences in median delay between stations of up to about 0.5 s are acceptable (Engdahl, 1999).

Station Chang Mai (CHG) is a good example of a station that could be an ideal surrogate to the primary IMS array station Chang Mai Array (CMAR) at a separation distance of 37 km. Figs. 3 and 4 show that, except for a perturbation in the time history of CHG in 1974, the median patterns in time and azimuth are virtually identical for these two stations. The CHG perturbation has little effect on our median analyses, but would need to be investigated if historical reference events observed by the station during that time period were to be used. We also note that there is a small difference of about 0.2 s in the amplitudes of the azimuthal medians between these two stations. These characteristics are further amplified in Fig. 5(a) and (b). These figures show that for CHG and CMAR the medians of P-residuals projected onto $5^\circ \times 5^\circ$ source patches (cf. Engdahl et al., 1998) at teleseismic distances are clearly azimuthally dependent and (except for amplitude) are well correlated. The coherence of the source patch medians between the two stations is demonstrated in Fig. 6. However, a regression line fitted to these data using the method of Press et al. (1992) has a slope of about 0.70, suggesting that CHG residuals are slightly earlier for fast arrivals and slightly later for slow arrivals by about 0.2 s. This could hardly be a property of the earth or an artifact of our methodology. We suspect that the very different methods used by analysts to read the data from these

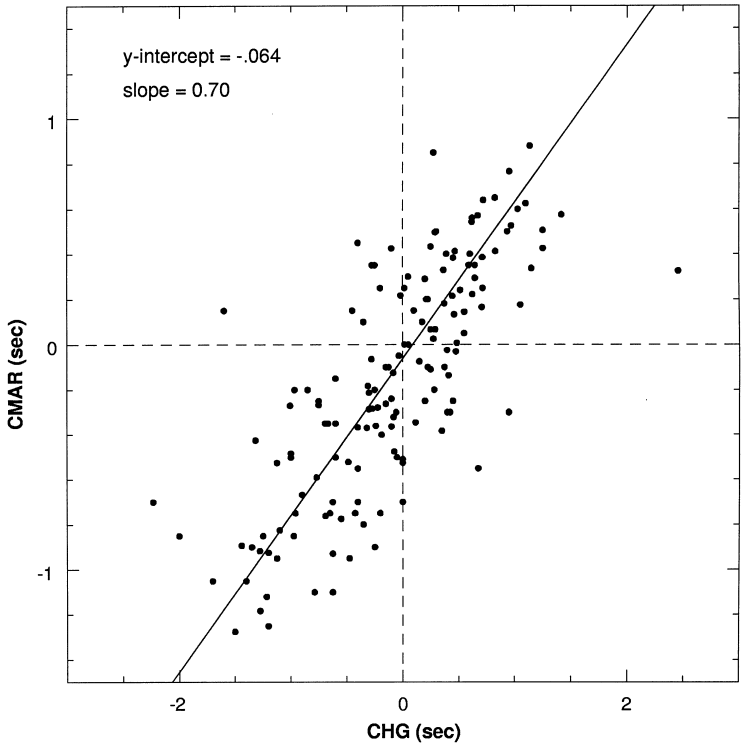

Fig. 6. Correlation of CHG and CMAR source patch medians.

two stations may be a factor. CHG has been read from paper WWSSN records at the station while data from CMAR are read interactively at the International Data Center from screen projections of the waveforms. The reduction in spread for CMAR median data is clearly a result of the more accurate picks that can be made in the latter case. But the improved signal-to-noise characteristics at the array CMAR could also result in the picking of earlier weaker signals at that station as compared to the corresponding later arriving picks at CHG. If this were the case, it could explain at least part of the rotation (from a slope of 1.0) of the regression line in Fig. 6.

2.5. Azimuthal variation of station medians

At each station, the travel time residuals display an azimuthal dependence due to the 3-D structure of the crust and mantle. The azimuthal variation of sector medians at station NRI is especially pronounced (Fig. 7(A)) reaching a peak to peak variation of over 4 s between sectors, which could reject this station from further analysis based on the previously set criteria. A projection of residuals to $5^\circ \times 5^\circ$ source patches (Fig. 8(a)) reveals, however, that positive residuals have their source along the north Atlantic ridge and Europe, whereas the larger negative residuals are produced by down going slabs in the western Pacific and Indonesia. The effects of slabs are not as pronounced for stations CHG and CMAR (Fig. 5) as it is likely that rays to those stations are not sampling the down going slabs as extensively as rays to NRI.

To remove the effects of 3-D mantle structure all NRI residuals were corrected by ray tracing through the 3-D P-model of Bijwaard et al. (1998). The resulting sector medians greatly reduce the azimuthal dependence of the NRI station medians (Figs. 7(B) and 8(b)), changing the grand median of the azimuthal sector medians from −0.45 to −1.20 s and reducing the spread from 1.41 to 0.30 s. Also brought into

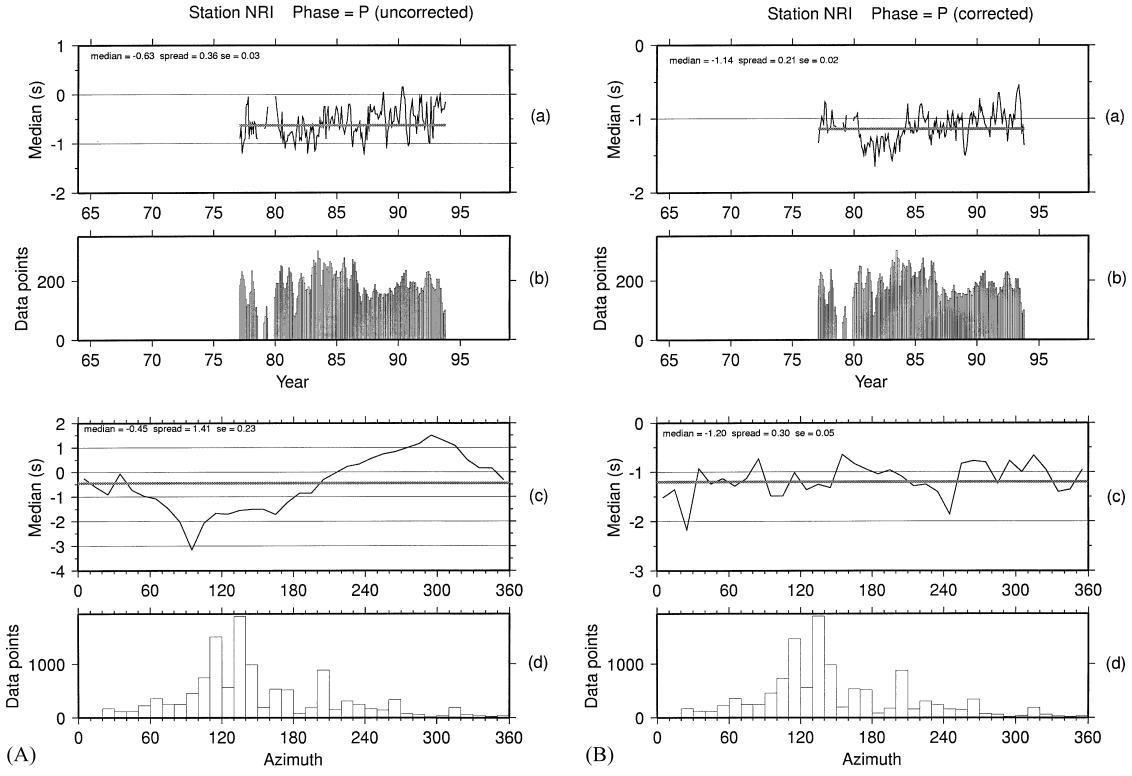

Fig. 7. Same as Fig. 1 but for teleseismic P-residual medians observed at station NRI (Norilsk, Russia). (A) Uncorrected and (B) corrected for 3-D source upper mantle, lower mantle and station upper mantle structure.

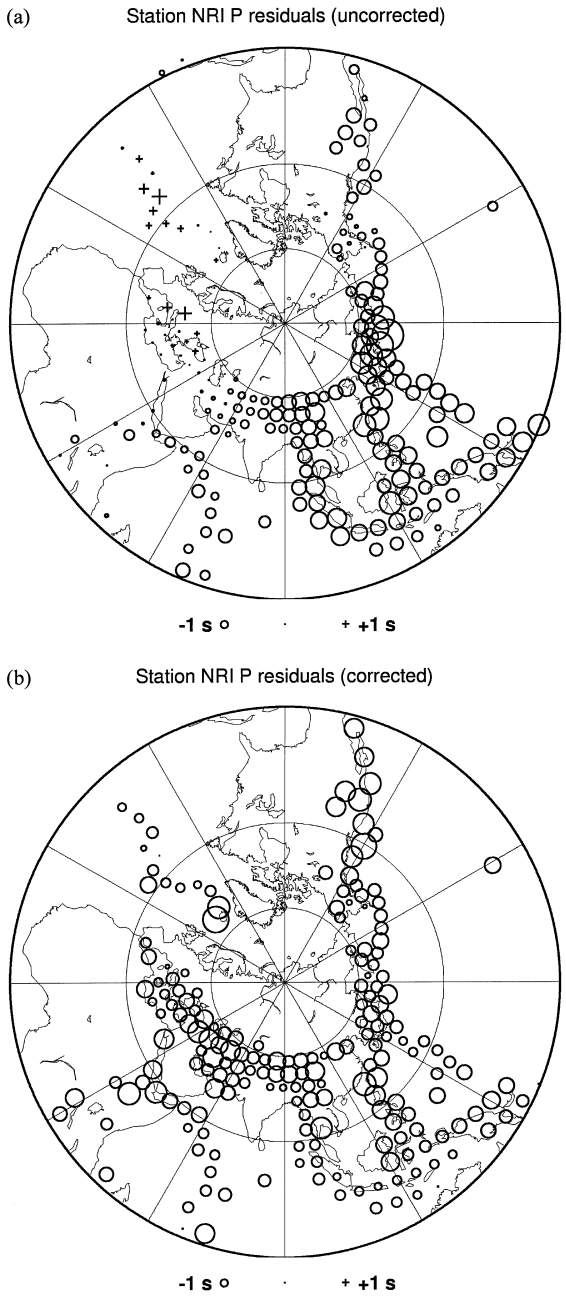

Fig. 8. Source patch (5° × 5° grid) medians of residuals for P-rays bottoming in the lower mantle observed at station NRI. (a) Uncorrected and (b) corrected for high-resolution 3-D source upper mantle, lower mantle and station upper mantle structure (below 400 km).

better focus is a possible problem in the time history of NRI during the period 1980–1984. The same analysis for station CHG changes the grand median of the azimuthal sector medians from −0.10 to −0.84 s and reduces the spread from 0.89 to 0.57 s and for station CMAR changes the grand median from −0.25 to −1.01 and reduces the spread from 0.52 to 0.37.

2.6. Correcting for near source and lower mantle structure

We have shown that in order to properly estimate crust and upper mantle station delays to stations NRI, CHG and CMAR it is necessary to remove the effects of source and lower mantle signatures in the residuals due to 3-D structure. Corrections for these effects typically have to be made for nearly all Eurasian stations. Hence, we use the 3-D high-resolution P- and S-wave models of Bijwaard et al. (1998) and Bijwaard (1999), respectively to remove the near source and lower mantle effects of 3-D structure from all Eurasian station residuals. These models are represented as perturbations to the 1-D reference model ak135 (Kennett et al., 1995). Because we aim to use P- and S-station delays to calibrate a Eurasian 3-D upper mantle model and S/P delay time ratio estimates to help merge the S- and P-parts of the model, station residuals are corrected from the source to a depth of 400 km beneath the station. At this depth and using the selection criteria previously described, upcoming teleseismic P-waves enter the model at distances between 1.4° and 3.5° and teleseismic S-waves between 1.5° and 3.3° from the station, respectively. At a depth of 200 km the annulus distances are less than half of these numbers. Hence, we conclude that the station delays we have estimated are representative of the integrated effects of all lateral heterogeneity within the limited region of the Eurasian upper mantle sampled by each station and within the resolution length (∼200 km) of 3-D upper mantle models (e.g. Villasenor et al., 2000) for the region.

3. Results

3.1. P- and S-station delays

Median P- and S-station delays are compared in Figs. 9 and 10 to a shear velocity model (Vsv)

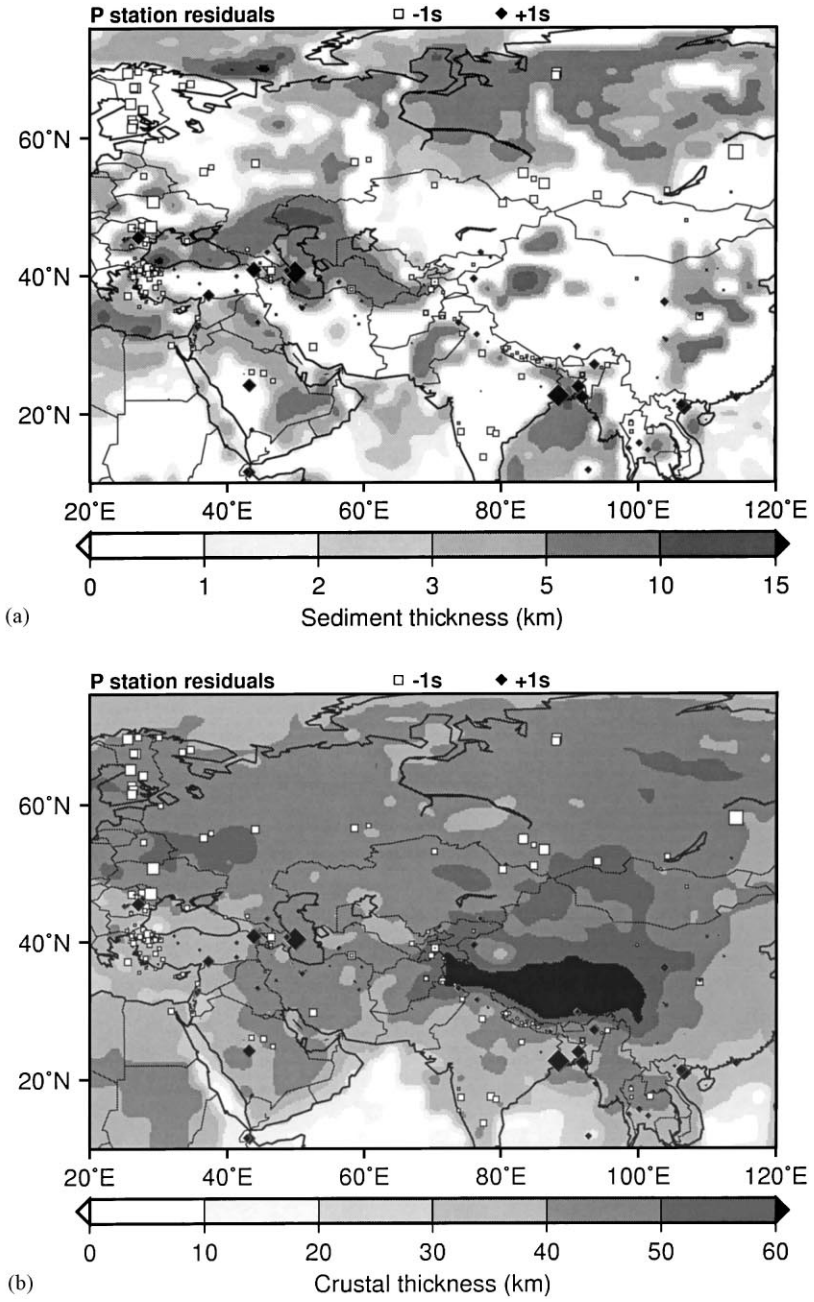

Fig. 9. P-station delays compared to tomographic imaging of (a) sediment thickness; (b) crustal thickness; and (c) shear velocity structure (Vsv) in the uppermost mantle at 100 km depth (positive velocity perturbations are contoured). Black diamonds indicate scaled slow delays and open squares scaled fast delays.

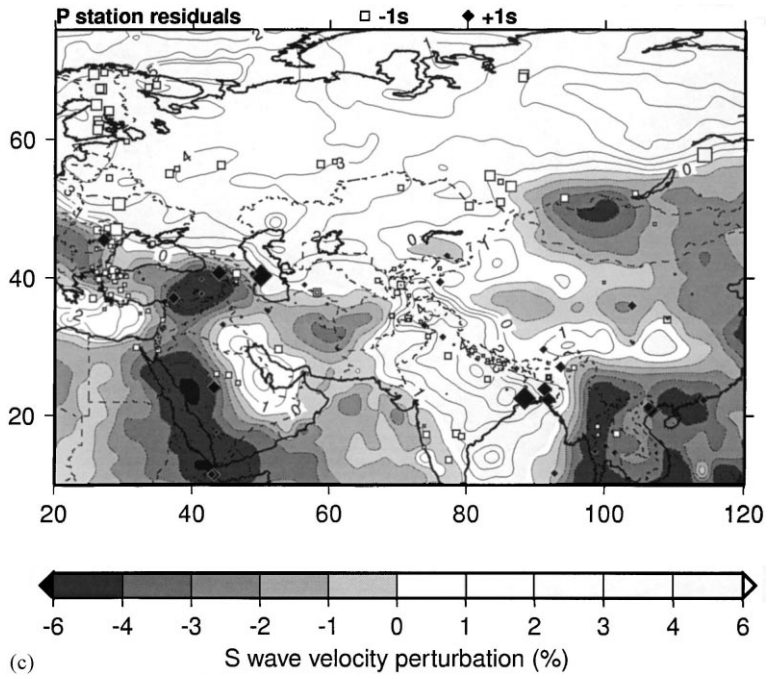

Fig. 9 (*Continued*).

of sediment thickness, crustal thickness, and upper mantle velocity structure, Vsv, at a depth of 100 km obtained by Villasenor et al. (2000) for central Eurasia. The model, parameterized in terms of velocity depth profiles on a discrete $2^\circ \times 2^\circ$ grid, was obtained by simultaneous inversion of broadband group and phase velocity maps of fundamental-mode Love and Rayleigh waves using a priori models for the crustal and sedimentary layers as starting models for the inversion procedure.

The P- and S-station delays correlate well with known tectonic features, such as sedimentary basins, cratons and orogens, the most obvious being fast delays associated with higher, upper mantle shear wave velocity anomalies beneath the east European platform, Siberian platform, and northern Indian shield. Some prominent groups of positive S-station delays (Fig. 10(a)) appear to be associated with large sedimentary basins along the Caucasus, the Turkmen/Tajik region, and near the eastern margin of India (the Ganges fan). Correlation of station delays with crustal thickness is not as obvious and perhaps is limited by the poor station coverage of regions that do have thickened crust such as the Tibetan plateau. However, there is one cluster of positive S-delays in the Tien Shan region (Fig. 10(b)) for which the only correlations that can be made are 40–50 km of thickened crust in the Vsv model (Fig. 10(b)) and a small low velocity anomaly in the uppermost mantle just north of the cluster (Fig. 10(c)). This latter anomaly is more prominent in the higher resolution 3-D P-model of Bijwaard (2000) who used a block sizes as small as 60 km in the region, suggesting that the feature may not be as well resolved by surface wave modeling. By far the best correlation are P-station delays associated with large low velocity mantle anomalies underlying the western Arabian peninsula, Red Sea, and the Afar triangle region in northeast Africa (Fig. 10(c)). The pattern of positive and negative P delays agrees exceptionally well with the apparent boundaries for these shear velocity anomalies in the upper mantle of the model. Both P- and S-station delays also correlate well with large low velocity regions of the upper mantle beneath Indochina and Mongolia southwest of Lake Baikal.

Fig. 11 compares the S-station delays to delays computed by integrating through the Vsv model

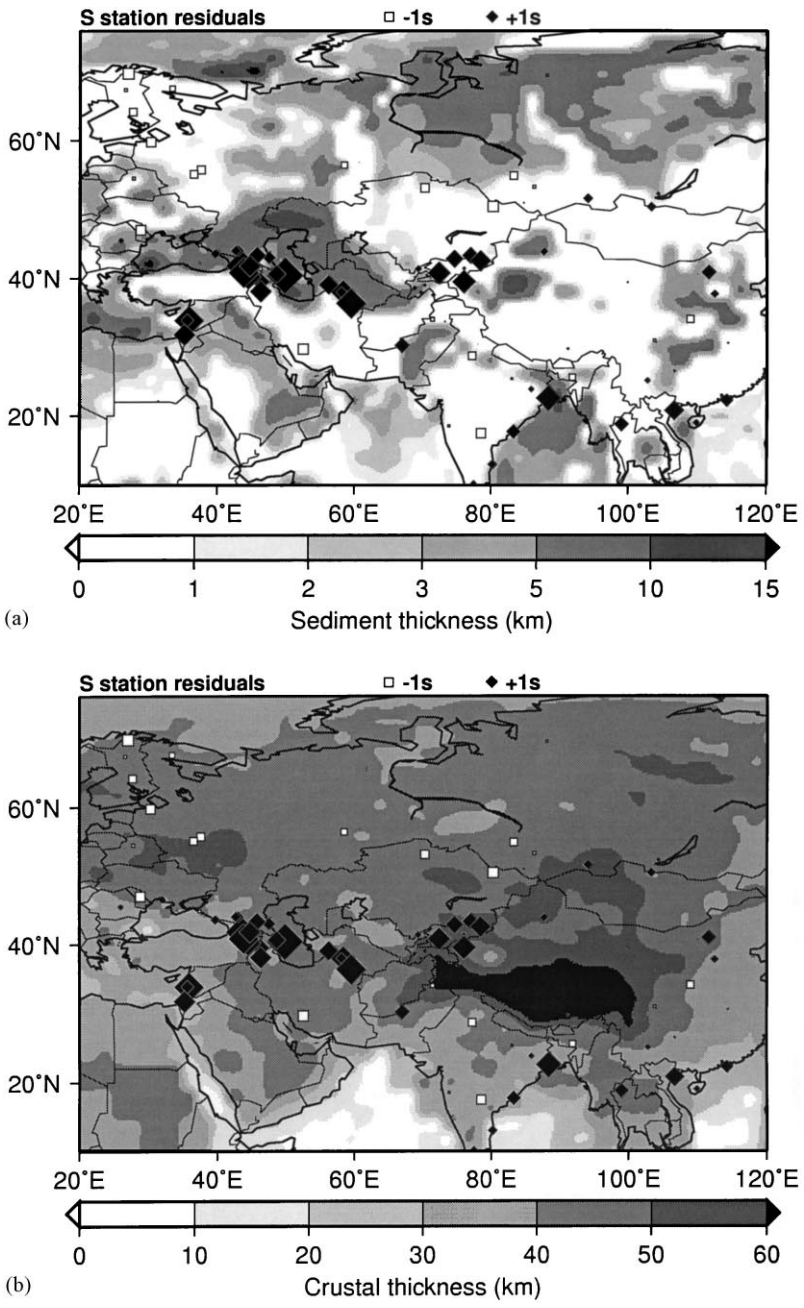

Fig. 10. S-station delays compared to the same tomographic images as Fig. 9.

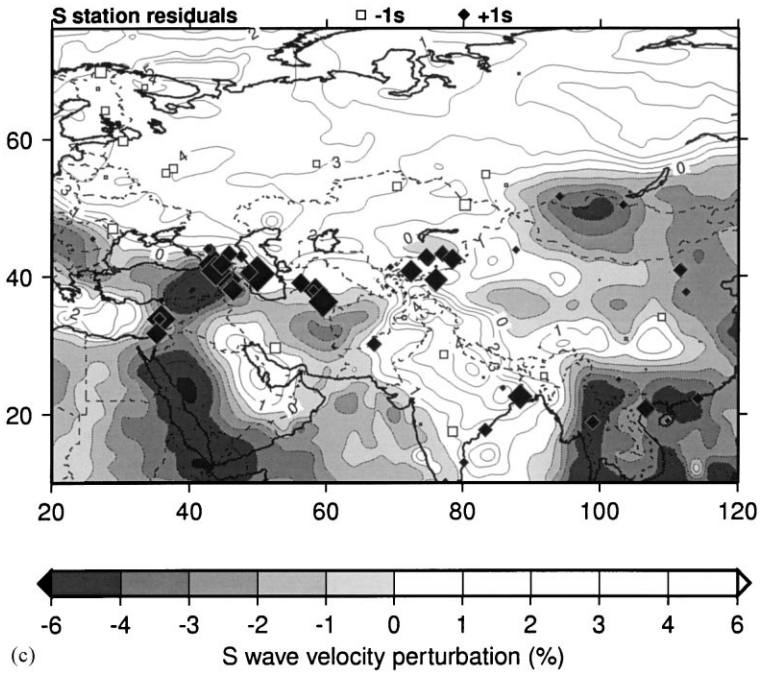

Fig. 10 (*Continued*).

beneath each station along a vertical path. While there is a general correlation between these delays there is also considerable scatter, undoubtedly due to the differences in resolution between the two data sets. The Eurasian Vsv model, presented in smoothed form in Figs. 9 and 10, has a resolution of only 200–300 km and the uncertainties in the predicted station delays are presently unknown. On the other hand, the S-station delays determined in this study have uncertainties of only several tenths of seconds and are based on the travel times of waves with wavelengths on the order of tens of kilometers. Hence, while sharp structural features in the real earth such as discontinuities or thickened sediments of small spatial extent may be seen in the station delays based on higher frequency waves, they would not necessarily be reflected in the predicted model delays.

3.2. S/P delay time ratio

Fig. 12 displays paired S- and P-station delays for Asian stations. A line of slope 1.9 (the S/P delay time ratio) was fitted using the method outlined by Press et al. (1992) that utilizes error estimates in both coordinates. Here we use the spread in each P and S-delay measurement as the estimated error. Because of the scatter, there is substantial uncertainty in this estimate of the S/P ratio. Nevertheless, our result is not inconsistent with the findings of Kennett et al. (1998) who performed a joint inversion of the Engdahl et al. (1998) P- and S-delays for 3-D P- and S-wave velocity variations globally. By taking the logarithmic derivatives of the velocity variations they found an S/P ratio of 1.9 to 2.2 throughout the uppermost mantle.

The offset of the correlation line could be caused by a baseline difference between the reference model (ak135) P- and/or S-upper mantle velocities and the real velocities beneath Eurasia. The most likely explanation is that S-wave velocities are slower on average in the regions sampled by our station delays as compared to S-wave velocities in the reference model (ak135). The scatter in Fig. 12 may have several sources. In addition to the basic reading error, the reported S-arrivals may have been read from vertical component seismograms at some stations and horizontal components at others and the procedures at any

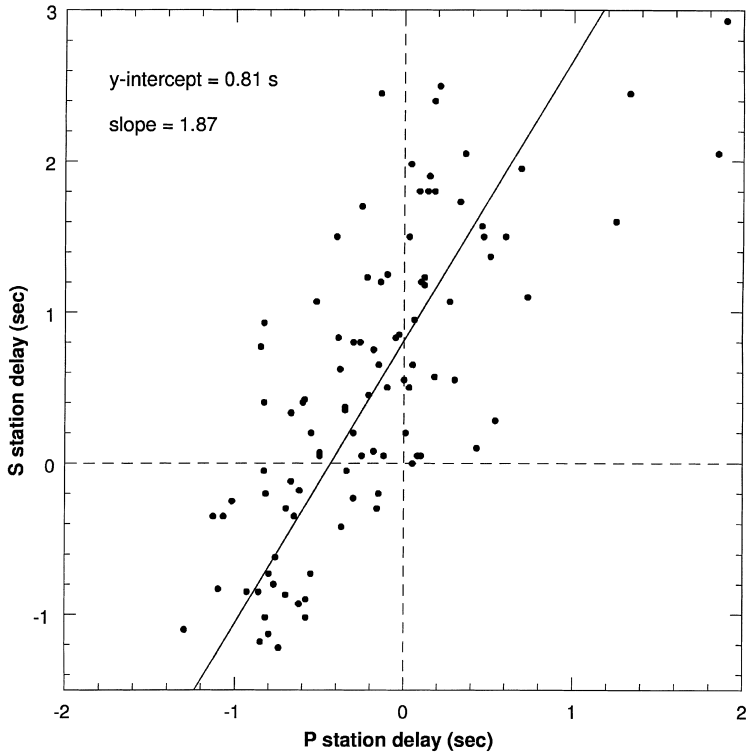

Fig. 11. Correlation between P- and S-delay times with a slope of about 1.9.

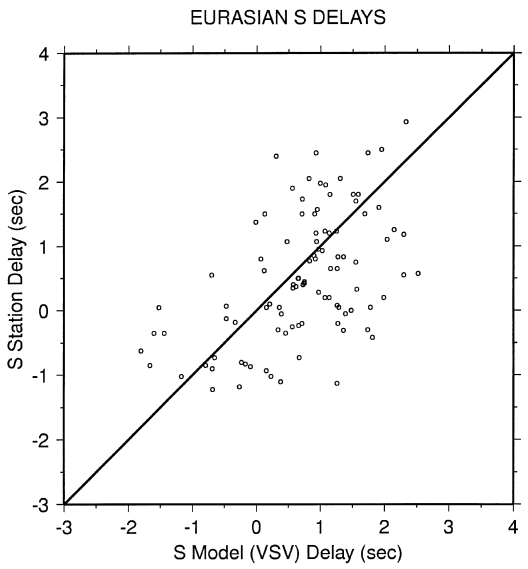

Fig. 12. S-station delays compared to delays computed by integrating through a Eurasian Vsv model (Vsv) beneath each station along a vertical path.

given station may change with time as well. There is, however, a possibility that P- and S-wave velocities in some parts of the 3-D Eurasian model may not be correlated, i.e. lateral variations in S-velocities do not exactly match those in P. In that case, station P- and S-delays rather than S/P delay time ratios could be more important for model validation.

4. Conclusions and discussion

We have demonstrated an approach that can be used to make robust estimates of P- and S-median delays for structure underlying Eurasian stations. This approach, which is based on the azimuthal binning of residuals, isolates the true delay in the crust and upper mantle beneath the station by minimizing the effects of temporal variations in station performance and the occurrence of earthquakes globally, and of 3-D structure outside the region of interest. Nevertheless, there remain variations in residuals as a function

of distance within individual azimuth sectors that are not fully accounted for. Figs. 5 and 6, even though uncorrected for global 3-D structure, suggest that the grand median of source patch medians may be an even better way to obtain unbiased estimates of P- and S-station delays. A grand median of −0.15 s for 206 uncorrected CHG source patch medians (Fig. 5(a)) is in excellent agreement with a grand median of −0.18 s for 164 uncorrected source patch medians of its surrogate station CMAR (Fig. 5(b)). However, a similar analysis of 196 NRI source patch medians that have been corrected for global 3-D structure (Fig. 8(b)) gives a grand median of −1.62 as compared to the grand median of NRI azimuthal sectors of −1.20 s (Fig. 7(B)). We suspect that this difference may be due to underestimation of the amplitude of the 3-D wave speed anomalies for down going slabs that are sampled extensively by ray paths to station NRI. This underestimation of velocities can result from the heavy damping used in the global inversions, especially for the S-model of Bijwaard (1999). The source patch median approach obviously needs further study.

The azimuthal variations of the station median shown for station NRI (Figs. 7(A) and 8(a)) also point to a potential problem in prior estimates of station corrections that include azimuthal terms. Dziewonski and Anderson (1983) in a global study estimated station corrections based on three terms: a constant and two cosine terms in azimuth (θ), $\cos(\theta)$ and $\cos(2\theta)$, with appropriate phase shifts. The $\cos(\theta)$ terms tended to show an intriguing pattern of having the slow direction point towards the ocean for many stations near a coast and the $\cos(2\theta)$ terms showed stronger regional trends. However, as we have shown for station NRI and have observed for many other Eurasian stations, source-region upper mantle and lower mantle path 3-D structure can strongly map into these azimuthal terms.

The final corrected P- and S-station median station delays appear to be spatially coherent and well correlated qualitatively to tectonic features, and to structural elements of a new 3-D uppermost mantle model for central Eurasia developed from surface wave data (Villasenor et al., 2000). Estimates of S/P delay time ratios for paired station delays are generally correlated, but the origin of large observed variations from the general trend is not clear.

Acknowledgements

We thank Antonio Villasenor for the GMT script used to construct most of the figures shown in this paper and Ray Buland for the computer program used for robust median statistics. We are grateful to Cliff Thurber and Hans Israelson for helpful reviews. This work has been supported by contracts DTRA01-99-C-0019 and DTRA01-00-C-0013.

References

Bijwaard, H., 1999. Seismic travel-time tomography for detailed global mantle structure. University of Utrecht, Utrecht, The Netherlands, 179 pp.

Bijwaard, H., Spakman, W., Engdahl, E.R., 1998. Closing the gap between regional and global travel time tomography. J. Geophys. Res. 103, 30055–30078.

Dziewonski, A.M., Anderson, D.L., 1983. Travel times and station corrections for P waves at teleseismic distances. J. Geophys. Res. 88, 3295–3314.

Engdahl, E.R., 1999. Calibration of the IMS seismic network by surrogate stations. Seism. Res. Lett. 70, 227 (Abstract).

Engdahl, E.R., Van der Hilst, R.D., Buland, R.P., 1998. Global teleseismic earthquake relocation with improved travel times and procedures for depth determination. Bull. Seism. Soc. Am. 88, 722–743.

Kennett, B.L.N., Engdahl, E.R., Buland, R., 1995. Constraints on seismic velocities in the Earth from traveltimes. Geophys. J. Int. 122, 108–124.

Kennett, B.L.N., Widiyantoro, S., van der Hilst, R.D., 1998. Joint seismic tomography for bulk sound and shear wave speed in the Earth's mantle. J. Geophys. Res. 103 (12), 12469–12493.

Press, W.H., Teukolsky, S.A., Vetererling, W.T., Flannery, B.P., Numerical Recipes in C: The Art of Scientific Computing, 2nd Edition. Cambridge University Press, New York, 1992.

Roehm, A.H.E., Trampert, J., Paulssen, H., Snieder, R.K., 1999. Bias in reported seismic arrival times deduced from the ISC Bulletin. Geophys. J. Int. 137, 163–174.

Villasenor, A., Ritzwoller, M.H., Levshin, A.L., Barmin, M.P., Engdahl, E.R., Spakman, W., Trampert, J., 2000. Shear velocity structure of central Eurasia from inversion of surface wave velocities.. Phys. Earth Planet. Interiors 123, 169–184.